Induction of autophagy in ESCRT mutants is an adaptive response for cell survival in *C. elegans*

Abderazak Djeddi[1,*], Xavier Michelet[1,*], Emmanuel Culetto[1,*], Adriana Alberti[1], Nicolas Barois[2] and Renaud Legouis[1,‡]

[1]Centre de Génétique Moléculaire, UPR 3404, CNRS, Associée à l'université Paris-Sud XI, FRC3115, Avenue de la terrasse, Gif-sur-Yvette, 91198, France
[2]Institut des Sciences du Végétal, UPR2355, Avenue de la terrasse, Gif-sur-Yvette, 91198, France

*These authors contributed equally to the work
‡Author for correspondence (legouis@cgm.cnrs-gif.fr)

Accepted 19 September 2011
Journal of Cell Science 125, 685–694

doi: 10.1242/jcs.091702

Summary

Endosomes and autophagosomes are two vesicular compartments involved in the degradation and recycling of cellular material. They both undergo a maturation process and finally fuse with the lysosome. In mammals, the convergence between endosomes and autophagosomes is a multistep process that can generate intermediate vesicles named amphisomes. Using knockdowns and mutants of the ESCRT machinery (ESCRT-0–ESCRT-III, ATPase VPS-4) and the autophagic pathway (LGG-1, LGG-2, ATG-7, TOR), we analyzed in vivo the functional links between endosomal maturation and autophagy in *Caenorhabditis elegans*. We report here that, despite a strong heterogeneity of their developmental phenotypes, all ESCRT mutants present an accumulation of abnormal endosomes and autophagosomes. We show that this accumulation of autophagosomes is secondary to the formation of enlarged endosomes and is due to the induction of the autophagic flux and not a blockage of fusion with lysosomes. We demonstrate that the induction of autophagy is not responsible for the lethality of ESCRT mutants but has a protective role on cellular degradation. We also show that increasing the basal level of autophagy reduces the formation of enlarged endosomes in ESCRT mutants. Together, our data indicate that the induction of autophagy is a protective response against the formation of an abnormal vesicular compartment.

Key words: Endosomal maturation, Autophagosomes, Amphisomes, vpsE, *C.elegans*, LGG-1/Atg8

Introduction

The degradation and recycling of the cellular materials is essential for the cell to maintain its homeostasis. The endosomes and autophagosomes form a very complex and dynamic vesicular system whose final destination is the lysosome. Autophagy, which usually refers to macroautophagy, allows the degradation of cytoplasmic constituents, long-lived proteins and organelles, either by selective or non-selective sequestration (Reggiori and Klionsky, 2002; Yoshimori, 2004). Numerous studies have highlighted the large variety of physiological and pathophysiological roles of autophagy (Mizushima et al., 2008), such as developmental processes, cell death, anti-aging, antigen presentation, elimination of microorganisms and tumour suppression. In numerous human pathologies, an increased level of autophagy appears to be an adaptive process with a protective role for the organism (e.g. clearance of protein aggregates). However, in some situations the contribution of autophagy could be deleterious and an excess of 'self-eating' could trigger cell death (Levine and Kroemer, 2008). One of the key regulators of autophagy is the Target of Rapamycin (TOR) kinase, which represses the autophagic process in normal growing conditions, but other signalling molecules are also involved in this induction (Codogno and Meijer, 2005). Autophagy-inducing stimuli, such as starvation, trigger the nucleation and the elongation of a vesicle in which cytoplasmic constituents are sequestered by a flat isolation membrane, also called the phagophore, which could originate from the endoplasmic reticulum (Hayashi-Nishino et al., 2009; Yla-Anttila et al., 2009), the mitochondria (Hailey et al., 2010) or the plasma membrane (Ravikumar et al., 2010). Complete sequestration is achieved by the closure of the phagophore, resulting in the double-membrane autophagosome. In the next step, the autophagosomes fuse with lysosomes to form the autophagolysosomes, where the inner membrane and the cytoplasmic content are degraded. In yeast, the autophagosomes can only fuse with the vacuole (the lysosome counterpart) but in mammalian cells the maturation of autophagosomes appears to be dependent on the endo-lysosomal vesicular system (Eskelinen, 2005; Fader and Colombo, 2009). Autophagosomes are able to fuse with early (Liou et al., 1997; Tooze et al., 1990) and late endosomes (Berg et al., 1998; Fader et al., 2009), generating an intermediate compartment called amphisome, but also fuse directly with lysosomes (Dunn, 1990). From these observations it has been proposed that the maturation of autophagosomes could be a multistep process involving successive fusion events between autophagic vacuoles and the endo-lysosomal compartment (Berg et al., 1998; Eskelinen, 2005; Fader and Colombo, 2009).

The endosomal system allows the sorting of membrane proteins to the lysosome for degradation (Lemmon and Traub, 2000). The degradation of membrane proteins is triggered by mono-ubiquitylation and subsequent delivery of cargoes to

the intralumenal vesicles (ILV) of a particular endosomal compartment called the multi-vesicular body (MVB). Ultimately, ILVs are degraded after fusion with the lysosome (Gruenberg and Stenmark, 2004; Piper and Katzmann, 2007). Recent studies in the nematode, fly and mammals have shown that mutations in the endosomal sorting complexes required for transport (ESCRT) block endosomal maturation but also lead to an increased number of autophagosomes (Michelet et al., 2009; Michelet et al., 2010; Roudier et al., 2005; Rusten et al., 2007a; Rusten and Stenmark, 2009). The ESCRT machinery is composed of four complexes, ESCRT-0 to ESCRT-III, which are essential for the formation of ILVs in the MVB compartment and for the sorting of ubiquitylated membrane proteins. The current model for the function of the ESCRT machinery proposes that ESCRT-0, also called the Vps27/Hse-1 complex, is dedicated to the formation of cargoes of ubiquitylated proteins at the endosomal membrane. ESCRT-0 can recruit ESCRT-I via a direct interaction between Vps27/Hrs and Vps23/TSG101 (Bache et al., 2003; Katzmann et al., 2003; Lu et al., 2003) and ESCRT-II interacts with ESCRT-I through the binding of Vps36/EAP45 to Vps28 (Im and Hurley, 2008). Recent data, obtained using giant unilamellar vesicles, suggests that ESCRT-I and ESCRT-II are crucial for formation of the ILVs (Wollert and Hurley, 2010). The oligomerization of the coiled-coil proteins forming the ESCRT-III complex is then required for the scission of the ILVs. During the addressing of cargoes to the ILVs, ubiquitin is removed by the deubiquitinase Doa4. Finally, the ESCRT machinery is dissociated from the endosomal membrane by the ATPase Vps4 (Babst, 2005; Hurley and Emr, 2006).

The ESCRT machinery is highly conserved from yeast to humans, but its complexity has increased with the evolution of multicellular organisms, and several ESCRT-encoding genes have been duplicated in mammals and plants. Depletion of ESCRT proteins affects the maturation of endosomes and results in a common cellular phenotype, the formation of an expanded endosomal structure without ILV, called the class E compartment (Hurley and Hanson, 2010; Katzmann et al., 2002; Rodahl et al., 2009; Roudier et al., 2005; Shim et al., 2006). Although all yeast ESCRT mutants are viable (Raymond et al., 1992), inactivation in metazoans (fly, mouse, nematode) of several ESCRT components is lethal during development (Michelet et al., 2010). However, there is a very high level of heterogeneity of the developmental phenotypes and the inactivation of the same gene in different species can result in different phenotypes. Recent reports in fly, nematode and mammalian cells have revealed that the inactivation of certain ESCRT-encoding genes could result in an accumulation of both autophagosomal structures and abnormal endosomes (Lee et al., 2007; Michelet et al., 2009; Roudier et al., 2005; Rusten et al., 2007a). Three main hypotheses could explain the link between endocytosis and autophagy involving the ESCRT machinery (Rusten and Stenmark, 2009). First, the accumulation of autophagosomes could result from a defective fusion between autophagosomes and endo-lysosomes. Second, the ESCRT machinery could have a direct role in the formation or closure of the autophagosomes. Third, an increase in the autophagic flux could be a secondary response to a homeostasis deregulation in ESCRT mutants.

In this report, we take advantage of the nematode *Caenorhabditis elegans* to study the functional link between autophagosomes and endosomes during development. *C. elegans* only possess one homologue for each ESCRT component and we analyzed the autophagic process after depletion of the ESCRT components. Our results indicate that the individual depletion of almost all ESCRT components results in the formation of enlarged endosomes and, subsequently, the accumulation of autophagosomes. However, the stage of apparition of these vesicular defects and the developmental phenotype varies greatly between ESCRT components. We show that the accumulation of autophagosomes, but not the formation of enlarged endosomes, is correlated with the stage of lethality. We also report the first evidence of amphisomes in *C. elegans*, but they are not accumulated in ESCRT mutants. Genetic and cellular analyzes suggest that the formation of enlarged endosomes induces an increase in the autophagic flux to degrade this abnormal compartment. Finally, we demonstrate that the accumulation of autophagosomes is not responsible for the lethality but is a protective response to promote cell survival and maintain homeostasis.

Results

ESCRT mutants present heterogeneity in developmental phenotypes, but similarities in cellular defects

We have previously characterised the VPS-27 (ESCRT-0) and VPS-32 (ESCRT-III) proteins in *C. elegans*, and shown that their depletion resulted in larval and embryonic lethality, respectively, with the formation of enlarged endosomes and the accumulation of autophagosomes (Michelet et al., 2009; Roudier et al., 2005). However, the relationships between these phenotypes have not been further analyzed and the interactions between autophagosomes and endosomes have not yet been studied in the nematode. To study whether both phenotypes were a common feature of ESCRT components, we used an RNA interference (RNAi) approach to deplete the maternal and the zygotic contribution of 11 *vpsE* genes that cover all ESCRT complexes and the ATPase VPS-4, involved in ESCRT disassembly (Table 1). We observed that the developmental phenotypes of *vpsE* genes could be classified into three categories: embryonic lethality (*vps-32*), larval lethality (*vps-23*, *vps-27*, *vps-24*, *vps-4*, *vps-28*, *vps-37*) and no developmental lethality (*vps-20*, *vps-22*, *vps-25*, *pqn-19*) (Table 1). Noticeably, the depletion of components of the same ESCRT complex does not result in a similar developmental arrest. When available, we also analyzed the phenotype of deletion mutants that were generated by the knockout consortia and compared this phenotype with the one obtained by RNAi (supplementary material Table S1). These analyzes confirm that developmental heterogeneity is an intrinsic characteristic of ESCRT mutants and does not simply rely on RNAi efficiency. Interestingly, despite a difference in the stages of lethality of ESCRT-depleted animals we observed a common and characteristic moulting defect phenotype in larval arrested animals (Fig. 1). Moreover, we also observed the presence of vacuolar structures, mainly in the epidermis, which were similar to the enlarged endosomes previously described (Michelet et al., 2009; Roudier et al., 2005). To check whether these vacuoles were enlarged endosomes, we then used a VPS-27::GFP fusion protein to specifically label the endosomal vesicles (Fig. 2A,A′), which was checked by electron microscopy. In the 11 *vpsE(RNAi)*-treated animals that we tested, we always observed the formation of VPS-27::GFP-positive enlarged endosomes (Table 1 and Fig. 2B), but the stage at which they appeared varied between genes. Moreover, except for *vps-32* animals, the enlarged endosomes systematically appeared much earlier than

Table 1. Stages of developmental arrest, formation of enlarged endosomes and increase in autophagy in ESCRT-depleted animals

Phenotype class	RNAi*	ESCRT complex	Stage of arrest†	VPS-27::GFP enlarged endosomes‡	GFP::LGG-1 puncta accumulation	GFP::LGG-2 puncta accumulation
Embryonic	vps-32	ESCRT-III	Mid-emb	Early emb	Early emb	Early emb
Larval	vps-27	ESCRT-0	L2/L3	n.a.	L1	L1
	vps-4	ATPase	L2	Mid-emb	L1	L1
	vps-23	ESCRT-I	L1 to L3	Mid-emb	L1	L1-L2
	vps-28	ESCRT-I	L2 to L4	Mid-emb	L1 to L2	L2 to L4
	vps-37	ESCRT-I	L2 to L4	Mid-emb	L1 to L2	L2 to L4
	vps-24	ESCRT-III	L4 to adult	Late emb	L3	L4
Adult	vps-20	ESCRT-III	No	Late emb	Adult	Adult
	vps-22	ESCRT-II	No	L4 to adult	Adult	Adult
	vps-25	ESCRT-II	No	Adult	Adult	Adult
	pqn-19	ESCRT-0	No	Late emb	Adult	Adult

*All RNAi clones were from J. Ahringer's library (Kamath et al., 2003) except for *vps-23(RNAi)*, which was from Open Biosystem (Huntsville, AL).
†Developmental RNAi phenotypes obtained by feeding.
‡VPS-27::GFP endosomes were qualified as enlarged when the lumen was clearly visible. The number and the size of the enlarged endosomes were not identical between *vpsE(RNAi)*. For *vps-20* and *pqn-19* only 10% of animals presented clearly enlarged endosomes.
Early emb, mid-emb and late emb indicate embryonic stages before, during or after the morphogenesis respectively. L1, L2, L3 and L4 indicate the four larval stages. 'No' indicates that animals reached adulthood and were fertile. n.a., not available.

the lethality stage. For several genes, the formation of enlarged endosomes preceded by more than 24 hours the stage of lethality, suggesting that it was not the direct cause of death (Table 1). Together, these data indicate that despite variability in developmental phenotypes, the ESCRT mutants present similar cellular defects and, in particular, the characteristic class E compartment. This demonstrates that in the nematode the whole ESCRT machinery is involved in endosomal maturation.

ESCRT mutants present an increase in the autophagic flux that correlates with their developmental arrest

Next, we analyzed the autophagosomal vesicles using LGG-1 and LGG-2, the two Atg8 homologues in the worm, which associate with the autophagosome membranes (Alberti et al., 2010; Melendez et al., 2003). We used confocal microscopy to analyze the localization of GFP::LGG-1 and GFP::LGG-2 and observed a punctate staining, which is a characteristic of the

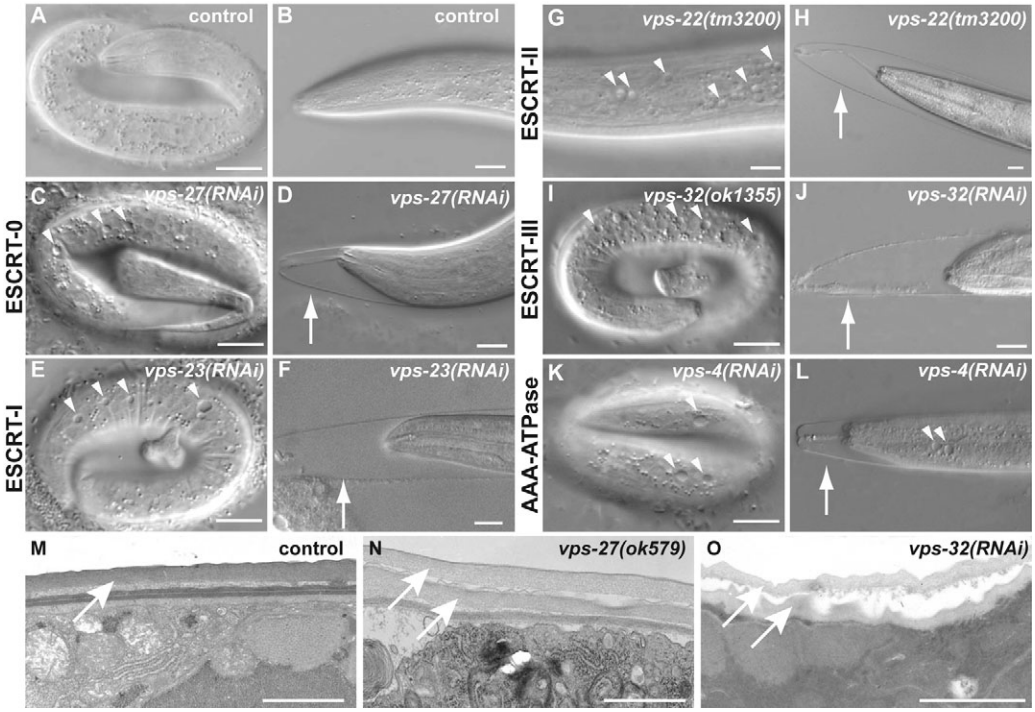

Fig. 1. ESCRT-depleted animals present epidermal defects. (**A**–**L**) Nomarski pictures of control embryo (A), control larva (B) and ESCRT-depleted animals (C–L). In ESCRT-depleted animals, cytoplasmic vacuoles (arrowheads) are present in the epidermis of embryos or larvae, which often appeared trapped in their old cuticle (arrows) indicating a moulting defect. (**M**–**O**) Electron micrographs of transversal section of the epidermis from control (M), *vps-27(ok579)* (N) and *vps-32(RNAi)* larvae (O). Arrows indicate the cuticular layers. Scale bars: 10 μm (A–L) and 1 μm (M–O).

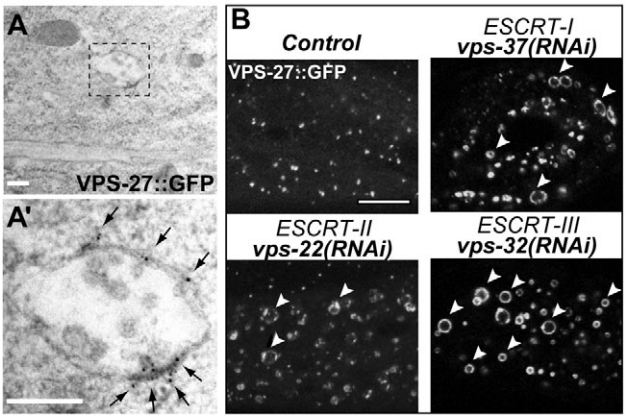

Fig. 2. ESCRT-depleted animals present enlarged endosomes. (**A**,**A′**) Electron microscopy images of control VPS-27::GFP worms incubated with anti-GFP antibody. Immuno-gold particles are observed at the surface of the endosome (black arrows) but not in internal vesicles. A′ is the magnification of the dotted square area in A. **(B)** Confocal fluorescent images of VPS-27::GFP in the epidermis of control, *vps-37(RNAi)*, *vps-22(RNAi)* and *vps-32(RNAi)* animals. White arrowheads point to enlarged endosomes in the epidermis of ESCRT-depleted animals. Scale bars: 200 nm (A, A′); 10 µm (B).

increase in autophagosomes (Alberti et al., 2010). For the 11 *vpsE(RNAi)* tested we observed an increase in the punctate staining with both GFP::LGG-1 and GFP::LGG-2 (Table 1 and Fig. 3A), suggesting that the depletion of ESCRT proteins leads to the accumulation of autophagosomal structures. To determine whether this increased number of autophagosomes results from an increase in the autophagic flux or a decrease in fusion with the lysosome, we next performed an immunoblotting analysis (Fig. 3B). This experiment allowed us to quantify both the post-translational modification of GFP::LGG-1, which corresponds to the phosphatidylethanolamine (PE)-conjugated form and the cleaved GFP form (Fig. 3C). It has been shown in yeast and in mammalian cells that Atg8/LC3-II inside autophagosomes is degraded by lysosomal hydrolases, after fusion of autophagosomes and lysosomes, and that the GFP fragment is relatively stable to proteolysis and therefore accumulates in an autophagy-dependent manner (Gutierrez et al., 2007; Hosokawa et al., 2006; Shintani and Klionsky, 2004). An increase in the GFP::LGG-1–PE and the cleaved GFP forms reflects an increase in the autophagic flux (Klionsky et al., 2008). Quantification by western blot demonstrated a strong enrichment of these two forms in *ESCRT(RNAi)* animals (Fig. 3B).

We also analyzed the *C. elegans* p62 homologue (T12G3.1), which is involved in autophagy during embryogenesis (Tian et al., 2010). P62 is a cargo adaptor protein that is involved in the addressing of aggregates to the autophagosomes and is degraded in the autophago-lysosome. In mammalian cells, it is a commonly used autophagic marker. Using confocal microscopy and immunoblotting, we analyzed T12G3.1::GFP in ESCRT-depleted animals and control animals (Fig. 3D,E). In *ESCRT(RNAi)* animals, T12G3.1::GFP presented a strongly punctate pattern and western blot analysis revealed that the cleaved GFP was also increased. This suggests that the autophagic flux was not blocked in ESCRT animals. Together these data indicate that the accumulation of autophagosomes in ESCRT-depleted animals is probably due to the increase in autophagic flux and not to the single blockage of fusion with lysosomes.

For the 11 *ESCRT(RNAi)* animals, we then analyzed at which developmental stage the accumulation of autophagosomes could first be observed and compared it with the stage of lethality and the stage of formation of enlarged endosomes (Table 1). This analysis revealed that the formation of enlarged endosomes was usually the first cellular defect in *ESCRT(RNAi)* animals and preceded the appearance of autophagic vesicles. This difference in the dynamics of alteration of the endosomal and autophagosomal vesicles suggests that the increase in autophagic flux is a secondary event. Interestingly, although we did not observed any obvious correlation between the formation of enlarged endosomes and the stages of lethality, the induction of autophagy was always observed after the formation of enlarged endosomes and increased until the stage of lethality. Together, these data suggest that the presence of enlarged endosomes is not lethal per se, but that the formation of this abnormal compartment could affect the cellular homeostasis and compromise developmental pathways.

There is no accumulation of amphisomes in *ESCRT(RNAi)* animals

Previous data from *Drosophila* suggests that the increase in autophagosomes in ESCRT mutants could be due to a blockage of fusion with the endo-lysosomal system (Rusten et al., 2007b). To test this hypothesis in *C. elegans*, we first analyzed whether the autophagosomes and the endosomes could fuse to generate amphisomes. Amphisomes are intermediate compartments that should have both endosomal and autophagic markers. Because amphisomes have not yet been studied in *C. elegans*, we first characterised them in wild-type embryos. Rusten and colleagues have shown that in the fat body of *Drosophila*, amphisomes were positive for both Hrs and GFP-tagged Atg8 (Rusten et al., 2007b) so we used immunofluorescence and confocal imaging to analyze the colocalization of the *C. elegans* homologues, namely VPS-27 and GFP::LGG-1. In wild-type embryos, VPS-27 and GFP::LGG-1 were very rarely detected on the same vesicle (0.09 double-positive vesicles per confocal plane) (Fig. 4A,C). We then performed the same analysis using VPS-32 and GFP::LGG-1 and also detected a very low level of colocalization (0.08 double-positive vesicles) (Fig. 4B,C). This result suggests that either the autophagic flux is fast and the amphisomes very transitory, or that the formation of amphisomes is a minority event and autophagosomes preferentially fuse directly with the lysosome. To check whether we would be able to detect an increase in the number of amphisomes, we performed the same analysis in a *rab-7(RNAi)* background. The small GTPase RAB-7 is involved in the fusion of both endosomes and autophagosomes with the lysosomes in mammals (Gutierrez et al., 2004; Jager et al., 2004; Meresse et al., 1995) and *C. elegans* (Alberti et al., 2010). In *rab-7(RNAi)* animals, we observed an accumulation of LGG-1 positive and VPS-27::GFP positive vesicles and a fivefold increase in the number of vesicles positive for both markers compared with the control (0.45 vesicles per confocal plane) (Fig. 4A,C). These data provide the first evidence for the presence of amphisomes in *C. elegans*. We then performed the same analysis in a *ESCRT(RNAi)* background by depleting either *vps-32* or *vps-4*. As expected, we detected the formation of enlarged vesicles and the accumulation of autophagosomes

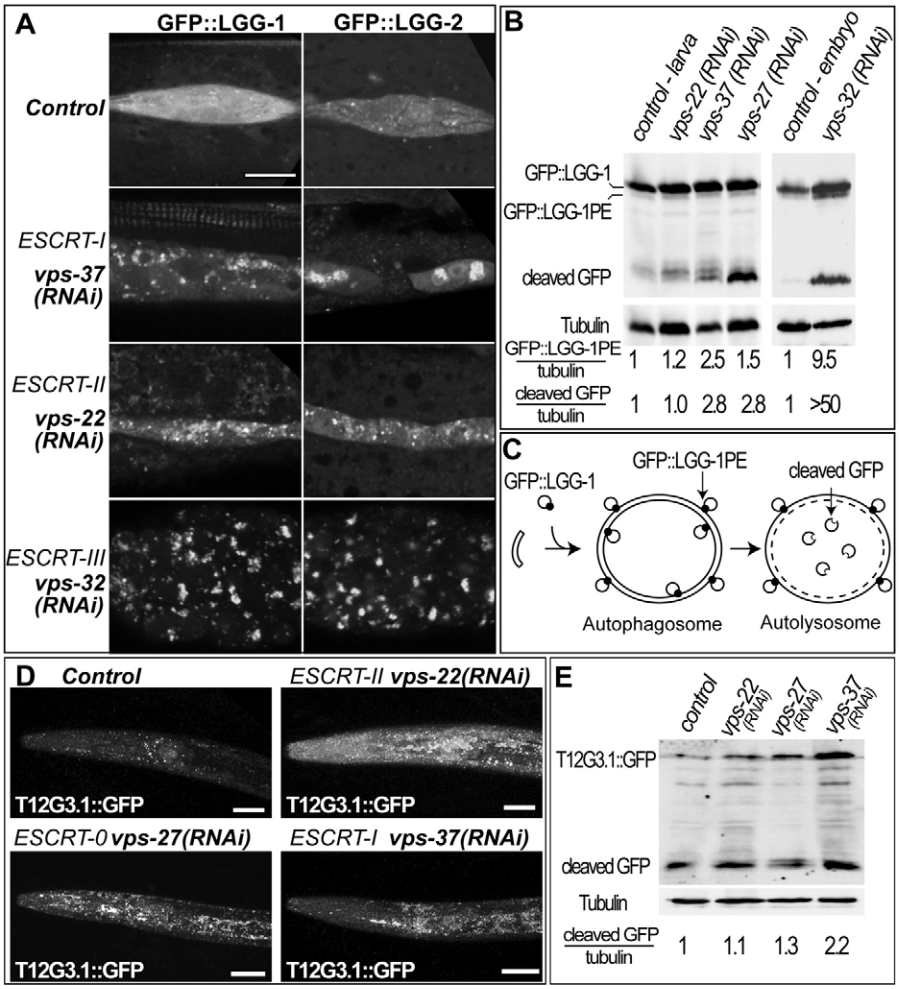

Fig. 3. ESCRT-depleted animals present an increase in the autophagic flux. (**A**) Confocal images of GFP::LGG-1 and GFP::LGG-2 in the epidermis of control (L3 stage), *vps-37(RNAi)* (L3 stage), *vps-22(RNAi)* (adult stage) and *vps-32(RNAi)* (embryo) animals. For *vps-37(RNAi)* and *vps-32(RNAi)* pictures have been captured at the stage where the animals arrest their development (see also Table 1). The increase of LGG-1 and LGG-2 positive dots indicates an increase in the number of autophagosomes. (**B**) Western blot of total protein extracts of synchronized GFP::LGG-1 transgenic worms incubated with anti-GFP antibodies. Both maternal and zygotic contribution was depleted by RNAi and synchronized worms were collected 48 hours after egg laying at the third larval stage, except for *vps-32(RNAi)* animals, which were collected as embryos. The cleaved GFP forms (around 28 kDa) correspond to the GFP degradation products in the autophagolysosome. To analyze the autophagic flux, the ratios of GFP::LGG-1PE to tubulin and of cleaved GFP to tubulin were quantified and normalized to the control. For *vps-37(RNAi)*, *vps-27(RNAi)* and *vps-32(RNAi)*, which were analyzed close to their developmental arrest, the quantification indicates an increase in the autophagic flux. For *vps-22(RNAi)* animals there was no larval lethality and no significant modification of the autophagic flux was detected at the L3 stage. (**C**) Representation of the autophagic flux. GFP::LGG-1 is present in the cytosol and after conjugation with PE (GFP::LGG-1PE) it becomes associated with the membrane of the autophagosomes. Then, fusion with the lysosome to form an autolysosome results in acidification and the release of a GFP fragment (cleaved GFP). (**D**) Confocal projections of T12G3.1::GFP (p62 homologue) in the head of control, *vps-37(RNAi)*, *vps-22(RNAi)* and *vps-27(RNAi)* larvae (L3 or L4). The increased number of structures positive for the adapter protein p62 indicates an increase in the number of autophagosomes. (**E**) Western blot of total protein extracts of synchronized T12G3.1::GFP transgenic worms incubated with anti-GFP antibodies. Synchronized larvae were collected 48 hours after egg laying. The presence of the cleaved GFP form suggests that fusion between autophagosomes and lysosomes does occur in ESCRT-depleted animals. Quantification of the cleaved GFP to tubulin ratio supports the notion that the autophagic flux is functional and increased in ESCRT mutants. Scale bars: 10 μm (A); 20 μm (D).

(Fig. 4A,B) but quantification of the colocalization revealed no increase in the number of amphisomes (0.07 and 0.03 double-positive vesicles per confocal plane, respectively) (Fig. 4C). Similarly, we observed no accumulation of vesicles positive for both VPS-32 and GFP::LGG-1 in *vps-4(RNAi)* animals (0.09 double-positive vesicles per confocal plane) (Fig. 4B,C). Together these results suggest that the depletion of the ESCRT machinery leads to an increase in autophagy but does not result in the accumulation of amphisomes.

The increase in autophagic flux is not responsible for lethality in ESCRT mutants.

To analyze whether the increase in autophagic flux could be responsible for the lethality of ESCRT-depleted animals, we performed a genetic analysis to modify the level of autophagy in various ESCRT mutants. We first focused on *vps-32(ok1355)*, *vps-27(ok579)* and *vps-36(tm1483)* mutants, which die at the first (L1), second (L2) or fourth (L4) larval stages, respectively, and used RNAi to either decrease the autophagic process

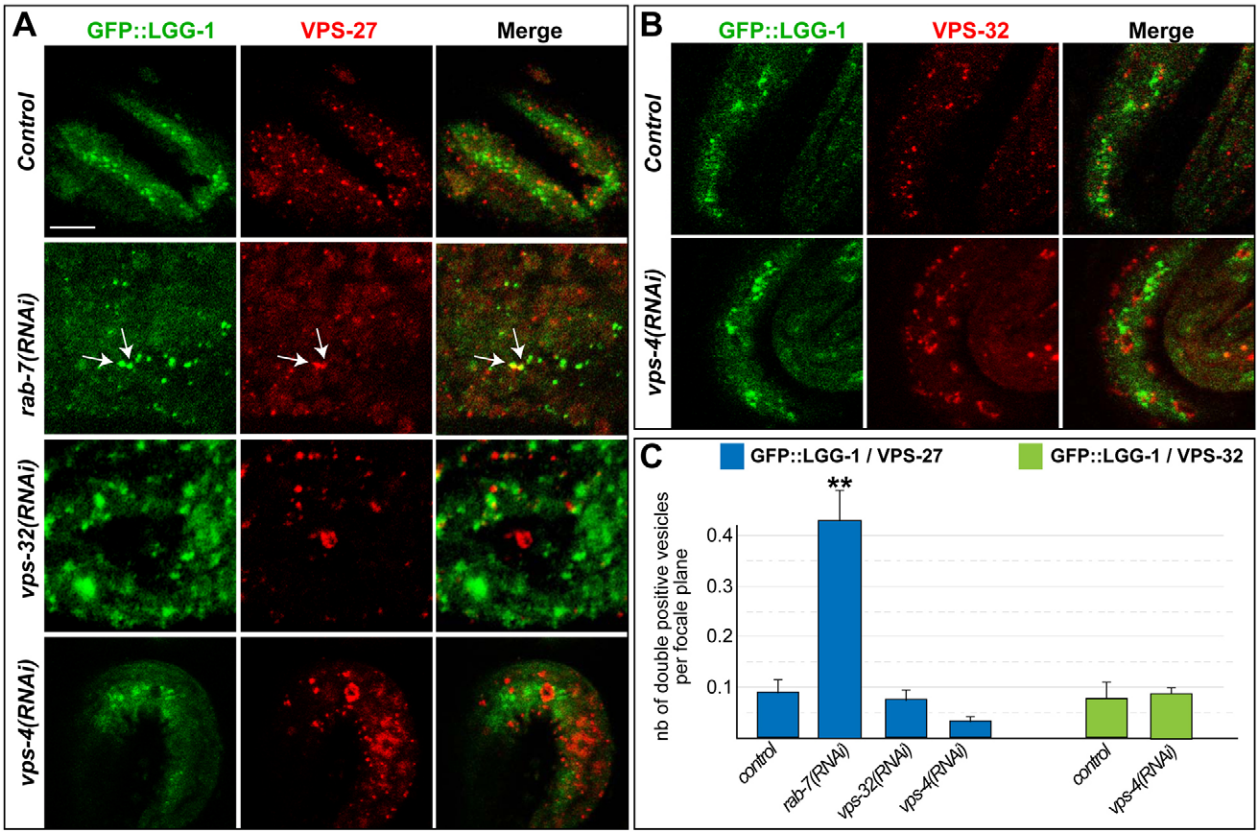

Fig. 4. Amphisomes are not accumulated in ESCRT-depleted animals. (**A**,**B**) Immunostaining with anti-VPS-27 (A) or anti-VPS-32 (B) (red) and anti-GFP (green) antibodies of *gfp::lgg-1* control, *rab-7(RNAi)*, *vps-32(RNAi)* and *vps-4(RNAi)* embryos. Each picture represents a single confocal plane of the embryos. In *rab-7(RNAi)*, the size of autophagosomal (green) and endosomal (red) vesicles appears slightly increased and the amphisomes (white arrows) are more numerous. In ESCRT-depleted embryos, enlarged endosomes and autophagosomes were present but amphisomes were not accumulated. Scale bar: 10 µm. (**C**) Quantification of the number of vesicles positive for both LGG-1 and VPS-27 (blue bars) or LGG-1 and VPS-32 (green bars). In control and ESCRT-depleted embryos, the level of amphisomes was very low but was increased fivefold in *rab-7(RNAi)* embryos. The numbers of confocal sections and embryos analyzed were for LGG-1/VPS-27: control 320 and 12, *rab-7(RNAi)* 112 and 5, *vps-32(RNAi)* 201 and 9, *vps-4(RNAi)* 35 and 2; and for LGG-1/VPS-32: control 76 and 3, *vps-4(RNAi)* 46 and 2. Values indicate means + s.e.m. $^{**}P<0.01$ compared with control, using the Student's *t*-test.

[*lgg-1+2(RNAi)* or *atg-7(RNAi)*], or increase the autophagic flux [*TOR(RNAi)*] (see supplementary material Fig. S1 for a control of induction) (Neufeld, 2010). Because these ESCRT mutations are lethal, we grew heterozygous animals in control or RNAi conditions and analyzed the stage of the lethality of the homozygous progeny (Table 2). We observed that neither the decrease nor the increase of the autophagic process was able to rescue the lethality of ESCRT mutants. However, we observed that *vps-27(ok579) lgg-1+2(RNAi)* animals died more precociously (L1 instead of L2) than *vps-27(ok579)* animals. These results indicate that the induction of autophagy is not responsible of the lethality of ESCRT mutants and that blocking the autophagic process can aggravate ESCRT phenotypes. To confirm these results, we used *TOR(h111)* mutant animals, in which autophagy is constitutively induced, and analyzed the phenotypes of *vps-27*, *vps-32* and *vps-4* knockdowns (Table 2). The comparison of heterozygous and homozygous TOR-depleted animals revealed that the increase in the basal level of autophagy was able to delay the stage of lethality of *ESCRT(RNAi)* animals. Taken together, our data demonstrate that increasing the level of autophagy is beneficial for ESCRT-depleted animals and suggests that autophagy has a protective role.

Constitutive induction of autophagy reduces endosomal defects in ESCRT mutants

We then asked whether the increase of autophagy aims to counterbalance the cellular defects in ESCRT-depleted animals. Using Nomarski microscopy we compared the level of vacuolization in the epidermis of *vps-32(ok1355)* and *vps-27(ok579)* animals in standard, low or high levels of autophagy (Fig. 5). Heterozygous animals were grown on either control RNAi, *lgg-1+2 (RNAi)*, *atg-7(RNAi)* or *TOR(RNAi)* and the vacuolization of the epidermis was observed in the progeny. Homozygous animals for *vps-32(ok1355)* and *vps-27(ok579)* were analyzed before the stage of lethality. On control RNAi, a small number of vacuoles were observed for *vps-32(ok1355)* and *vps-27(ok579)* animals (Fig. 5A,E). However, the number of vacuoles strongly increased when autophagy was blocked (Fig. 5B,C,F,G) and almost disappeared when the basal level of autophagy was increased (Fig. 5D,H), demonstrating that the autophagy flux influences the formation of vacuoles in the epidermis of ESCRT-depleted animals. Previous reports have shown that these vacuoles correspond to enlarged endosomes and were positive for VPS-27::GFP (Michelet et al., 2009; Roudier et al., 2005). To check whether the accumulation of enlarged

Table 2. Autophagy is not responsible for the lethality of ESCRT-depleted animals

Genotypes	RNAi	Phenotype	%	*n*
*vps-27(ok579)**	Control	L2 lethal	26	386
	lgg-1+2(RNAi)	L1 lethal	25	495
	atg-7(RNAi)	L2 lethal	23	455
	TOR(RNAi)	L2 lethal	23	479
vps-32(ok1355)†	Control	L1 lethal	23	372
	lgg-1+2(RNAi)	L1 lethal	23	537
	atg-7(RNAi)	L1 lethal	21	456
	TOR(RNAi)	L1 lethal	25	367
vps-36(tm1483)‡	Control	L4 lethal	25	289
	lgg-1+2(RNAi)	L4 lethal	22	373
	atg-7(RNAi)	L4 lethal	23	544
TOR(h111); TOR(+)§	Control	Wild-type	71	161
TOR(h111)§	Control	L3 arrest [TOR]§	29	66
TOR(h111); TOR(+)§	*vps-32(RNAi)*	Mid-embryo	73	53
TOR(h111)§	*vps-32(RNAi)*	Late embryo to L1	27	19
TOR(h111); TOR(+)§	*vps-27(RNAi)*	L2–L3 lethal	69	224
TOR(h111)§	*vps-27(RNAi)*	L3 arrest [TOR]§	31	101
TOR(h111); TOR(+)§	*vps-4(RNAi)*	L2 lethal	70	211
TOR(h111)§	*vps-4(RNAi)*	L3 arrest [TOR]§	30	91

*Progeny issued from *vps-27(ok579)/unc-24(e138)dpy-20(e1282)*.
†Progeny issued from *vps-32(ok1355)/dpy-10(e128)unc-4(e120)*.
‡Progeny issued from *vps-36(tm1483)/dpy-11(e224)unc-76(e911)*.
§Progeny issued from *let-363(h111) dpy-5(e61)I; sDp2 [I,f (let-363(+) dpy-5(+)]*. *TOR* has been previously identified as *let-363*. *sDp2* is a free partial duplication of chromosome I, maintained in ~70% of the progeny and lost in the remaining 30% which are *let-363(h111) dpy-5(e61)* homozygous.[TOR] animals present a characteristic intestinal phenotype, they are arrested at the L3 stage but live for several days.
n, number of progeny analyzed.

endosomes in ESCRT mutants is affected by the level of the autophagic process, we constructed a *vps-32(ok1355) VPS-27::GFP* strain. Heterozygous animals were grown on control RNAi, *lgg-1+2(RNAi)* or *TOR(RNAi)* and the VPS-27::GFP pattern was analyzed in *vps-32(ok1355)* homozygous embryos. With a basal level of autophagy, the formation of enlarged endosomal vesicles was observed in *vps-32(ok1355)* embryos and larvae (Fig. 6A and supplementary material Fig. S2). When autophagy was blocked by *lgg-1+2(RNAi)* treatment, in *vps-32(ok1355)* mutants we observed embryos where the abnormal endosomal compartments were further enlarged (Fig. 6B) and these structures strongly accumulated in the larva (supplementary material Fig. S2). Conversely, in *TOR(RNAi)* conditions, the size and number of abnormal endosomes was strongly reduced (Fig. 6C). To confirm this observation, we used spermidine to pharmacologically induce the autophagy process (Morselli et al., 2011). *vps-32(ok1355)* embryos were grown in presence of 0.4 mM spermidine and the formation of VPS-27::GFP enlarged endosomes was compared with control conditions. Quantification indicated a decreased number of *vps-32(ok1355)* embryos with enlarged endosomes (supplementary material Fig. S3), further demonstrating that autophagy induction reduces the endosomal defects. These data show a correlation between the level of autophagy and the accumulation of enlarged endosomes in ESCRT-depleted animals.

Together, our results demonstrate that the increase of the autophagic flux in ESCRT-depleted animals is an adaptive response to the formation of enlarged endosomes that aims to block their formation or to degrade this aberrant compartment.

Discussion

In this report we have shown that ESCRT mutants in *C. elegans* present similar cellular defects, namely an accumulation of enlarged endosomes, an increased level of autophagy and epidermal moulting defects, but a heterogeneity in the stages of developmental arrest. The similarity of the endosomal phenotype supports the notion that the canonical ESCRT pathway is strongly conserved in the nematode, but the developmental phenotypic heterogeneity contrasts with the yeast situation where all *vpsE* mutants are viable. One can postulate that the knockdown of each gene does not affect the endosomal maturation to the same extent and we have observed that in ESCRT mutants only a fraction of the endosomes will form an enlarged compartment. Therefore, the stage of the terminal phenotype of ESCRT mutants could be dependent on the level of alteration of the pathway. Differences in cell proliferation between the phenotypes of ESCRT mutants have also been recently reported in *Drosophila* mutants (Vaccari et al., 2009). Alternatively, we cannot exclude that some of the ESCRT-encoding genes have additional roles in *C. elegans*. A number of observations have indicated that ESCRT proteins could be involved in non-endosomal functions, including transcriptional regulation, cell cycle control, cell polarity and gene silencing (Michelet et al., 2010; Slagsvold et al., 2006).

Our results demonstrate that the lethality is not due to the increase of the autophagic process and suggest that the formation of enlarged endosomes is not lethal per se, but probably leads to an alteration in cell signalling during developmental processes, due to an endocytosis defect. Studies in *Drosophila* and mouse have demonstrated that numerous signalling pathways are deregulated in ESCRT mutants (Michelet et al., 2010; Vaccari et al., 2009) and a defect in cholesterol trafficking has been hypothesized to be responsible for the *vps-27* moulting defect in *C. elegans* (Roudier et al., 2005). We can only speculate that the level of alteration of cholesterol trafficking could explain the recurrence of the moulting defect and the different larval stage arrest of *C. elegans* ESCRT mutants.

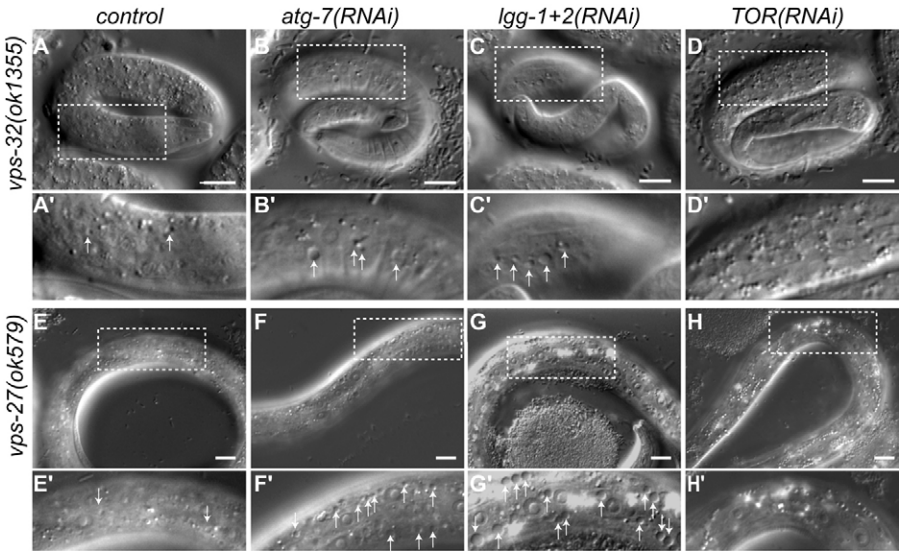

Fig. 5. Autophagy is protective of cellular degradation in ESCRT mutants. (**A**–**H′**) Nomarski pictures of *vps-32(ok1355)* and *vps-27(ok579)* mutants in control, decreased [*atg-7(RNAi)* or *lgg-1+lgg-2(RNAi)*] and increased [*TOR(RNAi)*] conditions of autophagy. Pictures correspond to the stages preceding developmental arrest of *vps-32(ok1355)* and *vps-27(ok579)* mutants, late embryo and L2, respectively. In ESCRT mutants, the degradation of the epidermis is shown by the formation of cytoplasmic vacuoles (white arrows). The blockage of the autophagic pathway results in an increase in the number and the size of the vacuoles whereas the constitutive induction suppresses this degradation. Scale bars: 10 μm. A′–H′ are twofold magnifications of the dotted areas in A–H.

This is the first report of the presence of amphisomes in the *C. elegans* embryo. At this stage, the autophagosomes are numerous but the number of amphisomes appear to be very low. Three hypotheses can explain such a low level. First, the fusion of amphisomes with lysosomes could be very fast. Second, only a subset of autophagosomes might form amphisomes while the rest fuse directly with lysosomes. Third, autophagosomes could fuse preferentially to fully mature MVBs and the resulting amphisomes would not be positive for either VPS-27 or VPS-32. In any case, formation of amphisomes in *C. elegans* appears to be intermediary between the situation in yeast in which no amphisome is formed and that in mammals where amphisomes originate from a multistep fusion procedure implicating early and late endosomes but also lysosomes (Berg et al., 1998; Eskelinen, 2005; Fader and Colombo, 2009).

Recent studies in HeLa cells have shown that autophagic degradation is inhibited in cells depleted of ESCRT subunits, suggesting that efficient autophagic degradation requires functional MVBs (Filimonenko et al., 2007; Tamai et al., 2007). Genetic mosaic analyses of ESCRT mutant cells in *Drosophila* have shown that a fusion defect between autophagic vesicles and the endo-lysosomal system is probably responsible for the accumulation of autophagosomes (Rusten et al., 2007b). In this report, we present three lines of evidence supporting the conclusion that the induction of autophagy in ESCRT mutants is an adaptive response for cell survival in *C. elegans*. First, the timing of the accumulation of enlarged endosomal vesicles and autophagic structures are different; second, the accumulation of autophagosomes is linked to an increase in the autophagic flux; and third, an increase in the basal level of autophagy partially rescues the endosomal phenotype whereas a blockage aggravates the formation of aberrant endosomes.

Like mammal and fly ESCRT mutants, the increase of autophagosomes in *C. elegans* appears to be a secondary consequence of the endosomal maturation defect. However, it corresponds to a physiological attempt to preserve cellular homeostasis and not an accumulation of immature autophagosomes. It is possible that differences in the autophagosome maturation process between worm, fly and mammals could explain this apparent discrepancy. One hypothesis is that the induction of autophagy in response to an endosomal defect is also present in fly and mammals but is masked because of the convergence of the two vesicular systems that

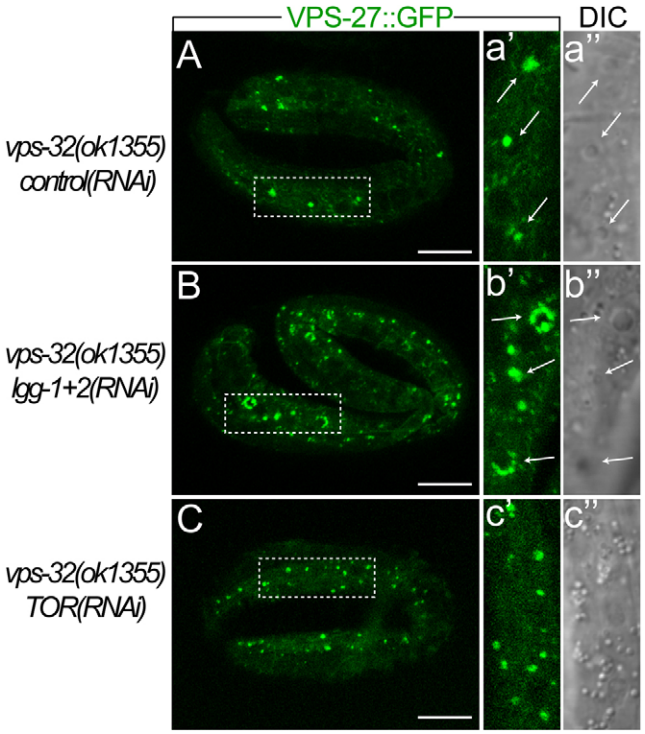

Fig. 6. Alterations in the level of autophagy modify the accumulation of enlarged endosomes in ESCRT mutants. (**A**–**C′**) Confocal and Nomarski images of VPS-27::GFP in the epidermis of *vps-32(ok1355)* mutants in control (A), decreased *lgg-1+lgg-2(RNAi)* (B), and increased *TOR(RNAi)* (C) conditions of autophagy. Pictures have been captured in late embryos, several hours before the stage when *vps-32(ok1355)* mutants stopped developing (L1 larva). Insets are twofold magnifications of GFP (a′–c′) or DIC (a″–c″) images of the areas indicated by dotted lines. The increase in the number and size of VPS-27::GFP enlarged vesicles (arrows) is visible in *lgg-1+lgg-2(RNAi)* embryos (B) compared with controls (A), but not in *TOR(RNAi)* embryos (C). Scale bars: 10 μm.

prevents the autophagosomes from completing their maturation. Our data suggest that in *C. elegans* the maturation of autophagosomes is less closely connected to endosomal maturation, which could explain the difference between *Drosophila* and HeLa cells with regard to the autophagic process (Filimonenko et al., 2007; Tamai et al., 2007). A recent report has shown that a dominant-negative mutation in CHMP2B (ESCRT-III), responsible for frontotemporal dementia, leads to an accumulation of autophagosomes in cortical neurons that is detrimental to neuronal survival (Lee and Gao, 2009). Interestingly, overexpression of the same mutation in hippocampal neurons does not result in an accumulation of autophagosomes (Belly et al., 2010). This suggests that, depending on the cell type, alteration of ESCRT components could have different effects on autophagy. In conclusion, our data form a new paradigm for the duality between the beneficial and detrimental effects of autophagy on cell survival.

Materials and Methods

C. elegans strains and genetic methods

Nematode strains were grown on NGM plates seeded with *E. coli* strain OP50 and handled as described (Brenner, 1974). The wild-type parent strain used was the *C. elegans* Bristol variety N2. Mutant alleles were provided by the *Caenorhabditis* Genetics Center at the University of Minnesota [*vps-27(ok579)*, *vps-32(ok1355)*, *alx-1(gk275)* , *alx-1(gk338)*, *alx-1(gk412)*, *pqn-19 (ok406)*, *mvb-12 (ok3482)*, *vps-20 (ok2425)* and *vps-37 (ok1538)*] and by Shohei Mitani at the Japanese National Bioresource Project for the nematode [*vps-36(tm1483)* and *vps-22 (tm3200)*]. Lethal mutants were out-crossed and maintained as heterozygous strains with the following genotypes: *vps-27(ok579)/unc-24(e138)dpy-20(e1282)*, *vps-32(ok1355)/dpy-10(e128)unc-4(e120)*, *vps-36(tm1483)/dpy-11(e224)unc-76(e911)*, *vps-36(gk427)/dpy-11(e224)unc-76(e911)*, *vps-22 (tm3200)/dpy-1(e1)unc-32(e189)*.

The strain DA2123, carrying the integrated array *adIs2122[gfp::lgg-1; rol-6(d)]*, was a gift from Chanhee Kang (University of Texas, Dallas, TX) and the T12G3.1::GFP was a gift from Hong Zhang (NIBS, Beijing, China). RD106 *Ex[vps-27::gfp; rol-6(su1006)]* and RD108 *Ex[gfp::lgg-2; rol-6(su1006)]* were constructed in previous studies (Alberti et al., 2010; Roudier et al., 2005). KR3875 [*let-363(h111)dpy-5(e61)I; sDp2(I;f)*] was kindly provided by Donald Riddle (University of British Columbia, Vancouver, Canada).

RNA-mediated interference and spermidine experiments

RNAi by feeding was performed as described (Kamath et al., 2003). Briefly, synchronized worms were placed onto IPTG-containing NGM plates seeded with bacteria (*E. coli HT115*[DE3]) carrying the empty vector L4440 (pPD129.36) as control or the bacterial clones from the J. Ahringer library, Open Biosystem (*vps-23*) or a gift from Malene Hansen, Sanford-Burnham Medical Research Institute, La Jolla, CA (*TOR*). RNAi phenotypes were scored in the F1 generation after bacterial feeding of L4 larvae for 2 days. To score *vps-32* larval RNAi phenotypes, L1 larvae were fed with the bacterial RNAi clone throughout larval development.

Spermidine plates were prepared as follows: 150 µl of *E.coli* overnight culture was spread on freshly poured 10 ml NGM plates and 2 hours later plates were exposed to a UV source for 10 minutes. 40 µl of spermidine solution (0.1 M) was diluted in a final volume of 250 µl, spread over the surface of the plate and allowed to diffuse overnight. Plates were used the following day.

Protein extraction and western blot analysis

To prepare total worm extracts, worm pellets were resuspended in PBS containing 2% Triton X-100 (Alberti et al., 2010). One volume of glass beads were added before homogenization using a Precellys24 instrument (Bertin Technologies) for two cycles of 60 seconds at 6000 r.p.m. Protein extracts were mixed with Laemli buffer, denatured for 5 minutes at 100°C and separated on a 15% SDS-polyacrylamide gel by electrophoresis. Proteins were transferred to nitrocellulose membranes (Whatman, Dassel, Germany), probed with the affinity-purified anti-GFP antibody (1:500; Roche) and revealed using horse radish peroxidase-conjugated antibodies (1:10,000; Promega) and the ECL detection system (SuperSignal pico Chemiluminescent Subsrate, Pierce, Rockford, IL). Signals were quantified on a Las3000 photoimager (Fuji) using ImageQuant 5.2 software (Molecular Dynamics).

Immunofluorescence microscopy

Embryos or larvae were prepared for antibody staining by freeze fracture and fixation in 2% PFA as previously described (Legouis et al., 2000). After a saturation step with 1× PBS, 2% BSA, 0.5% Triton X-100 for 20 minutes, samples were incubated in the same buffer overnight at room temperature with the following antibodies: rabbit polyclonal anti-VPS-32 at 1:2000, rabbit polyclonal anti-VPS-27 at 1:500 and mouse monoclonal anti-GFP at 1:250. Alexa-Fluor-488- and Alexa-Fluor-568-conjugated secondary antibodies (Molecular Probes) were used at 1:500. Routinely, fluorescent expression and phenotypic analyses were carried out on a Zeiss Axioskop2 Plus equipped with Nomarski optics coupled to a camera (CoolSNAP, Roper Scientific). Confocal images were captured on an inverted Leica TCSSP2 confocal microscope with a Z-step of 0.3–0.5 µm. Image analysis was performed with the ImageJ software (http://rsb.info.nih.gov/ij/). To quantify the colocalization between GFP::LGG-1 and either VPS-27 or VPS-32 we counted the number of vesicles that were positive for GFP::LGG-1 and VPS-27 or VPS-32 for each focal plane. For each condition, 2–12 embryos were imaged and 46–320 focal planes analyzed. All images were then processed with Adobe Photoshop Software and Adobe Illustrator.

Electron microscopy

Morphology analysis of larvae was performed as previously described (Legouis et al., 2000). Briefly, blocks of four to six animals were sectioned either transversely or longitudinally, postfixed with osmium tetroxyde and uranyl acetate, and stained with uranyl acetate and lead citrate. Then, 16 *vps-27(ok579)* L2 larvae and nine *vps-32* larval RNAi L4 animals were analyzed and compared with wild-type worms at corresponding stages. For immuno-electron microscopy, animals were transferred to 200-µm deep flat carriers, followed by cryo-immobilization in the EMPACT-2 HPF apparatus (Leica Microsystems) and cryo-substitution as described (Kolotuev et al., 2009). Ultrathin sections on formvar- or carbon-coated copper grids were sequentially treated for 10 minutes with 1% Tween20 and 100 mM glycine, and then with 1% BSA (all in 1× PBS). Samples were then labelled with the primary rabbit anti-GFP antibody (1:400 dilution; ab290, Abcam) and, after washes, labelled with the secondary goat anti-rabbit antibody coupled to 10 nm colloidal gold particles (1:20 dilution, BB International) both in 1× PBS containing 1% BSA for 30 minutes. After extensive washes, sections were contrasted with 2% uranyl acetate for 5 minutes. Sections were observed with a Jeol 1400 TEM at 120 kV and images acquired with a Gatan 11 Mpixels SC1000 Orius CCD camera.

Acknowledgements

We thank A. Prévot for technical assistance, Y. Schwab, B. Satiat-Jeunemaitre and C. Lefebvre for help in the microscopy analyses. We thank Donald Riddle, Malene Hansen, Shohei Mitani, Hong Zhang and the *Caenorhabditis* Genetic Center, which is funded by the NIH National Center for Research Resources (NCRR), for providing reagents. We are grateful to the members of the Legouis laboratory, Patrice Codogno and Vincent Galy for helpful discussions and Christopher J. Herbert for critical reading of the manuscript.

Funding

This work was supported by the Agence National de la Recherche, the Association pour la Recherche contre le Cancer. A.D. and X.M. are recipients of a fellowship from the Ministère de l'Education et de la Recherche Technologique and from the Association pour la Recherche contre le Cancer, respectively. The Imaging and Cell Biology facility of the IFR87 (FR-W2251) 'La plante et son environnement' is supported by the Action de Soutien à la Technologie et la Recherche en Essonne, Conseil de l'Essonne.

Supplementary material available online at
http://jcs.biologists.org/lookup/suppl/doi:10.1242/jcs.091702/-/DC1

References

Alberti, A., Michelet, X., Djeddi, A. and Legouis, R. (2010). The autophagosomal protein LGG-2 acts synergistically with LGG-1 in dauer formation and longevity in *C. elegans*. *Autophagy* **6**, 622-633.

Babst, M. (2005). A protein's final ESCRT. *Traffic* **6**, 2-9.

Bache, K. G., Brech, A., Mehlum, A. and Stenmark, H. (2003). Hrs regulates multivesicular body formation via ESCRT recruitment to endosomes. *J. Cell Biol.* **162**, 435-442.

Belly, A., Bodon, G., Blot, B., Bouron, A., Sadoul, R. and Goldberg, Y. (2010). CHMP2B mutants linked to frontotemporal dementia impair maturation of dendritic spines. *J. Cell Sci.* **123**, 2943-2954.

Berg, T. O., Fengsrud, M., Stromhaug, P. E., Berg, T. and Seglen, P. O. (1998). Isolation and characterization of rat liver amphisomes. Evidence for fusion of autophagosomes with both early and late endosomes. *J. Biol. Chem.* **273**, 21883-21892.

Brenner, S. (1974). The genetics of *Caenorhabditis elegans*. *Genetics* **77**, 71-94.
Codogno, P. and Meijer, A. J. (2005). Autophagy and signaling: their role in cell survival and cell death. *Cell Death Differ.* **12 Suppl. 2**, 1509-1518.
Dunn, W. A., Jr (1990). Studies on the mechanisms of autophagy: maturation of the autophagic vacuole. *J. Cell Biol.* **110**, 1935-1945.
Eskelinen, E. L. (2005). Maturation of autophagic vacuoles in mammalian cells. *Autophagy* **1**, 1-10.
Fader, C. M. and Colombo, M. I. (2009). Autophagy and multivesicular bodies: two closely related partners. *Cell Death Differ.* **16**, 70-78.
Fader, C. M., Sanchez, D. G., Mestre, M. B. and Colombo, M. I. (2009). TI-VAMP/VAMP7 and VAMP3/cellubrevin: two v-SNARE proteins involved in specific steps of the autophagy/multivesicular body pathways. *Biochim. Biophys. Acta.* **1793**, 1901-1916.
Filimonenko, M., Stuffers, S., Raiborg, C., Yamamoto, A., Malerod, L., Fisher, E. M., Isaacs, A., Brech, A., Stenmark, H. and Simonsen, A. (2007). Functional multivesicular bodies are required for autophagic clearance of protein aggregates associated with neurodegenerative disease. *J. Cell Biol.* **179**, 485-500.
Gruenberg, J. and Stenmark, H. (2004). The biogenesis of multivesicular endosomes. *Nat. Rev. Mol. Cell Biol.* **5**, 317-323.
Gutierrez, M. G., Munafo, D. B., Beron, W. and Colombo, M. I. (2004). Rab7 is required for the normal progression of the autophagic pathway in mammalian cells. *J. Cell Sci.* **117**, 2687-2697.
Gutierrez, M. G., Saka, H. A., Chinen, I., Zoppino, F. C., Yoshimori, T., Bocco, J. L. and Colombo, M. I. (2007). Protective role of autophagy against *Vibrio cholerae* cytolysin, a pore-forming toxin from *V. cholerae*. *Proc. Natl. Acad. Sci. USA* **104**, 1829-1834.
Hailey, D. W., Rambold, A. S., Satpute-Krishnan, P., Mitra, K., Sougrat, R., Kim, P. K. and Lippincott-Schwartz, J. (2010). Mitochondria supply membranes for autophagosome biogenesis during starvation. *Cell* **141**, 656-667.
Hayashi-Nishino, M., Fujita, N., Noda, T., Yamaguchi, A., Yoshimori, T. and Yamamoto, A. (2009). A subdomain of the endoplasmic reticulum forms a cradle for autophagosome formation. *Nat. Cell Biol.* **11**, 1433-1437.
Hosokawa, N., Hara, Y. and Mizushima, N. (2006). Generation of cell lines with tetracycline-regulated autophagy and a role for autophagy in controlling cell size. *FEBS Lett.* **580**, 2623-2629.
Hurley, J. H. and Emr, S. D. (2006). The ESCRT complexes: structure and mechanism of a membrane-trafficking network. *Annu. Rev. Biophys. Biomol. Struct.* **35**, 277-298.
Hurley, J. H. and Hanson, P. I. (2010). Membrane budding and scission by the ESCRT machinery: it's all in the neck. *Nat. Rev. Mol. Cell Biol.* **11**, 556-566.
Im, Y. J. and Hurley, J. H. (2008). Integrated structural model and membrane targeting mechanism of the human ESCRT-II complex. *Dev. Cell* **14**, 902-913.
Jager, S., Bucci, C., Tanida, I., Ueno, T., Kominami, E., Saftig, P. and Eskelinen, E. L. (2004). Role for Rab7 in maturation of late autophagic vacuoles. *J. Cell Sci.* **117**, 4837-4848.
Kamath, R. S., Fraser, A. G., Dong, Y., Poulin, G., Durbin, R., Gotta, M., Kanapin, A., Le Bot, N., Moreno, S., Sohrmann, M. et al. (2003). Systematic functional analysis of the *Caenorhabditis elegans* genome using RNAi. *Nature* **421**, 231-237.
Katzmann, D. J., Odorizzi, G. and Emr, S. D. (2002). Receptor downregulation and multivesicular-body sorting. *Nat. Rev. Mol. Cell Biol.* **3**, 893-905.
Katzmann, D. J., Stefan, C. J., Babst, M. and Emr, S. D. (2003). Vps27 recruits ESCRT machinery to endosomes during MVB sorting. *J. Cell Biol.* **162**, 413-423.
Klionsky, D. J., Abeliovich, H., Agostinis, P., Agrawal, D. K., Aliev, G., Askew, D. S., Baba, M., Baehrecke, E. H., Bahr, B. A., Ballabio, A. et al. (2008). Guidelines for the use and interpretation of assays for monitoring autophagy in higher eukaryotes. *Autophagy* **4**, 151-175.
Kolotuev, I., Schwab, Y. and Labouesse, M. (2009). A precise and rapid mapping protocol for correlative light and electron microscopy of small invertebrate organisms. *Biol. Cell* **102**, 121-132.
Lee, J. A. and Gao, F. B. (2009). Inhibition of autophagy induction delays neuronal cell loss caused by dysfunctional ESCRT-III in frontotemporal dementia. *J. Neurosci.* **29**, 8506-8511.
Lee, J. H., Koh, H., Kim, M., Kim, Y., Lee, S. Y., Karess, R. E., Lee, S. H., Shong, M., Kim, J. M., Kim, J. et al. (2007). Energy-dependent regulation of cell structure by AMP-activated protein kinase. *Nature* **447**, 1017-1020.
Legouis, R., Gansmuller, A., Sookhareea, S., Bosher, J. M., Baillie, D. L. and Labouesse, M. (2000). LET-413 is a basolateral protein required for the assembly of adherens junctions in *Caenorhabditis elegans*. *Nat. Cell Biol.* **2**, 415-422.
Lemmon, S. K. and Traub, L. M. (2000). Sorting in the endosomal system in yeast and animal cells. *Curr. Opin. Cell Biol.* **12**, 457-466.
Levine, B. and Kroemer, G. (2008). Autophagy in the pathogenesis of disease. *Cell* **132**, 27-42.
Liou, W., Geuze, H. J., Geelen, M. J. and Slot, J. W. (1997). The autophagic and endocytic pathways converge at the nascent autophagic vacuoles. *J. Cell Biol.* **136**, 61-70.
Lu, Q., Hope, L. W., Brasch, M., Reinhard, C. and Cohen, S. N. (2003). TSG101 interaction with HRS mediates endosomal trafficking and receptor down-regulation. *Proc. Natl. Acad. Sci. USA* **100**, 7626-7631.
Melendez, A., Talloczy, Z., Seaman, M., Eskelinen, E. L., Hall, D. H. and Levine, B. (2003). Autophagy genes are essential for dauer development and life-span extension in *C. elegans*. *Science* **301**, 1387-1391.
Meresse, S., Gorvel, J. P. and Chavrier, P. (1995). The rab7 GTPase resides on a vesicular compartment connected to lysosomes. *J. Cell Sci.* **108**, 3349-3358.
Michelet, X., Alberti, A., Benkemoun, L., Roudier, N., Lefebvre, C. and Legouis, R. (2009). The ESCRT-III protein CeVPS-32 is enriched in domains distinct from CeVPS-27 and CeVPS-23 at the endosomal membrane of epithelial cells. *Biol. Cell* **101**, 599-615.
Michelet, X., Djeddi, A. and Legouis, R. (2010). Developmental and cellular functions of ESCRT machinery in pluricellular organisms. *Biol. Cell* **102**, 191-202.
Mizushima, N., Levine, B., Cuervo, A. M. and Klionsky, D. J. (2008). Autophagy fights disease through cellular self-digestion. *Nature* **451**, 1069-1075.
Morselli, E., Marino, G., Bennetzen, M. V., Eisenberg, T., Megalou, E., Schroeder, S., Cabrera, S., Benit, P., Rustin, P., Criollo, A. et al. (2011). Spermidine and resveratrol induce autophagy by distinct pathways converging on the acetylproteome. *J. Cell Biol.* **192**, 615-629.
Neufeld, T. P. (2010). TOR-dependent control of autophagy: biting the hand that feeds. *Curr. Opin. Cell Biol.* **22**, 157-168.
Piper, R. C. and Katzmann, D. J. (2007). Biogenesis and function of multivesicular bodies. *Annu. Rev. Cell Dev. Biol.* **23**, 519-547.
Ravikumar, B., Moreau, K., Jahreiss, L., Puri, C. and Rubinsztein, D. C. (2010). Plasma membrane contributes to the formation of pre-autophagosomal structures. *Nat. Cell Biol.* **12**, 747-757.
Raymond, C. K., Howald-Stevenson, I., Vater, C. A. and Stevens, T. H. (1992). Morphological classification of the yeast vacuolar protein sorting mutants: evidence for a prevacuolar compartment in class E vps mutants. *Mol. Biol. Cell* **3**, 1389-1402.
Reggiori, F. and Klionsky, D. J. (2002). Autophagy in the eukaryotic cell. *Eukaryot. Cell* **1**, 11-21.
Rodahl, L. M., Haglund, K., Sem-Jacobsen, C., Wendler, F., Vincent, J. P., Lindmo, K., Rusten, T. E. and Stenmark, H. (2009). Disruption of Vps4 and JNK function in *Drosophila* causes tumour growth. *PLoS ONE* **4**, e4354.
Roudier, N., Lefebvre, C. and Legouis, R. (2005). CeVPS-27 is an endosomal protein required for the molting and the endocytic trafficking of the low-density lipoprotein receptor-related protein 1 in *Caenorhabditis elegans*. *Traffic* **6**, 695-705.
Rusten, T. E. and Stenmark, H. (2009). How do ESCRT proteins control autophagy? *J. Cell Sci.* **122**, 2179-2183.
Rusten, T. E., Filimonenko, M., Rodahl, L. M., Stenmark, H. and Simonsen, A. (2007a). ESCRTing autophagic clearance of aggregating proteins. *Autophagy* **4**, 233-236.
Rusten, T. E., Vaccari, T., Lindmo, K., Rodahl, L. M., Nezis, I. P., Sem-Jacobsen, C., Wendler, F., Vincent, J. P., Brech, A., Bilder, D. et al. (2007b). ESCRTs and Fab1 regulate distinct steps of autophagy. *Curr. Biol.* **17**, 1817-1825.
Shim, J. H., Xiao, C., Hayden, M. S., Lee, K. Y., Trombetta, E. S., Pypaert, M., Nara, A., Yoshimori, T., Wilm, B., Erdjument-Bromage, H. et al. (2006). CHMP5 is essential for late endosome function and down-regulation of receptor signaling during mouse embryogenesis. *J. Cell Biol.* **172**, 1045-1056.
Shintani, T. and Klionsky, D. J. (2004). Autophagy in health and disease: a double-edged sword. *Science* **306**, 990-995.
Slagsvold, T., Pattni, K., Malerod, L. and Stenmark, H. (2006). Endosomal and non-endosomal functions of ESCRT proteins. *Trends Cell Biol.* **16**, 317-326.
Tamai, K., Tanaka, N., Nara, A., Yamamoto, A., Nakagawa, I., Yoshimori, T., Ueno, Y., Shimosegawa, T. and Sugamura, K. (2007). Role of Hrs in maturation of autophagosomes in mammalian cells. *Biochem. Biophys. Res. Commun.* **360**, 721-727.
Tian, Y., Li, Z., Hu, W., Ren, H., Tian, E., Zhao, Y., Lu, Q., Huang, X., Yang, P., Li, X. et al. (2010). *C. elegans* screen identifies autophagy genes specific to multicellular organisms. *Cell* **141**, 1042-1055.
Tooze, J., Hollinshead, M., Ludwig, T., Howell, K., Hoflack, B. and Kern, H. (1990). In exocrine pancreas, the basolateral endocytic pathway converges with the autophagic pathway immediately after the early endosome. *J. Cell Biol.* **111**, 329-345.
Vaccari, T., Rusten, T. E., Menut, L., Nezis, I. P., Brech, A., Stenmark, H. and Bilder, D. (2009). Comparative analysis of ESCRT-I, ESCRT-II and ESCRT-III function in *Drosophila* by efficient isolation of ESCRT mutants. *J. Cell Sci.* **122**, 2413-2423.
Wollert, T. and Hurley, J. H. (2010). Molecular mechanism of multivesicular body biogenesis by ESCRT complexes. *Nature* **464**, 864-869.
Yla-Anttila, P., Vihinen, H., Jokitalo, E. and Eskelinen, E. L. (2009). 3D tomography reveals connections between the phagophore and endoplasmic reticulum. *Autophagy* **5**, 1180-1185.
Yoshimori, T. (2004). Autophagy: a regulated bulk degradation process inside cells. *Biochem. Biophys. Res. Commun.* **313**, 453-458.